8.9 EVALUATION OF SATELLITE AND RADAR CLOUD RETRIEVAL METHODS DURING IMPROVE-2 ICING EVENTS

Julie Haggerty*, J. Vivekanandan, and David Serke
National Center for Atmospheric Research, Boulder, Colorado

1. INTRODUCTION

Current techniques for detecting and forecasting the presence of aircraft icing conditions rely on radar, satellite, and surface observations as well as model predictions. Meteorological conditions related to aircraft icing are well-documented; both passive and active remote sensing techniques are useful for characterizing a subset of those conditions. Satellite-based methods using combinations of visible reflectance and infrared emittance detect supercooled liquid water near the tops of opaque clouds, and hence can provide useful information for icing detection schemes (Minnis et al., 2001; Vivekanandan et al., 1996). Radar retrieval methods that rely on fuzzy logic techniques yield particle habit classifications, providing further detail about cloud microphysical characteristics (Vivekandandan et al., 1999).

In this paper, satellite methods for estimating cloud thermodynamic phase and radar methods for identifying particle habit are applied to case studies from a recent field campaign. Each result is compared with coincident aircraft measurements of cloud bulk and microphysical properties. Consistency between satellite- and radar-derived properties is also examined.

2. DATA SET

The Improvement of Microphysical Parameterization through Observational Verification Experiment (IMPROVE) was designed to characterize a variety of precipitation systems in the Pacific Northwest region (Stoelinga et al., 2003). IMPROVE-2 focused on orographic lifting as a primary precipitation generating mechanism. Sixteen intensive observing periods were conducted utilizing a variety of measurement platforms including the University of Washington Convair-580, the NCAR S-band dual-polarization Doppler radar (S-Pol), and a scanning microwave radiometer. Coincident satellite data from the Advanced Very High Resolution Radiometer (AVHRR/3) on NOAA Polar Orbiting Environmental Satellites (POES) and the Geostationary Operational Environmental Satellite (GOES) Imager were obtained during this period.

* Corresponding author address: Julie A. Haggerty, National Center for Atmospheric Research, P.O. Box 3000, Boulder, CO 80307; email: haggerty@ucar.edu

Visible reflectance and infrared emittance measurements from AVHRR/3 and the GOES Imager are required for the satellite-based retrieval methods. Specific channels used for AVHRR-based cloud retrievals are at 0.63, 1.61, and 10.8 μm. Nominal spatial resolution at nadir is 1 km. Retrievals from the GOES Imager are based on 0.65, 3.9, 10.8, and 12.0 μm data. Spatial resolution is on the order 4 km. Imagery is available half-hourly.

The NCAR S-Pol radar was deployed in the lower western foothills of the Cascade Mountains. It was used for long-range weather surveillance and for directing aircraft into precipitation features. Observations of reflectivity, polarimetric and Doppler velocity structures of precipitation features that developed in the study area were obtained for selected case studies.

In situ measurements of cloud bulk and microphysical properties in icing conditions are essential for evaluating the efficacy of satellite- and radar-derived cloud and icing products. IMPROVE-2 provided an array of in-situ observations suitable for assessment of the techniques applied here. Specifically, liquid water content, particle size distributions, and particle phase information collected from Convair-580 sensors are used for comparison. These measurements were derived from a 2D-Cloud probe, Johnson-Williams and Gerber PVM-100A liquid water probes, and a Particle Measuring Systems FSSP-100 probe.

3. RETRIEVAL ALGORITHMS

3.1 *Radar Particle Identification*

The use of polarimeteric radar observables and derived fields for determination of liquid and ice hydrometeor characteristics including particle habits has been demonstrated by Vivekanandan et al. (1999). Their method relies on the relationships between microphysical properties and linear polarimetric observables including differential reflectivity (Z_{DR}), linear depolarization ratio (LDR), specific differential propagation phase (K_{DP}), and correlation coefficient (ρ_{HV}). For example, large LDR values are characteristic of tumbling, wet nonspherical particles, while small LDR values are associated with light rain, cloud droplets, and dry ice particles. The set of relationships between polarimetric radar observables and particle classes tend not to have hard boundaries, i.e., there is a fair amount of overlap between polarimetric observables for various particle types. For this reason, Vivekanandan et al. (1999) applied fuzzy

logic methods to develop a particle classification method.

For this analysis, the particle identification (PID) script is applied to raw range height indicator (RHI) data. Ancillary data including temperature profiles from mobile sonde data is incorporated in the process. Two graphical output formats are generated using results from the PID scheme. For each radar field a vertical cross-section parallel to the flight path and a constant altitude projection at flight level are produced, enabling comparison with aircraft and satellite data.

3.2 *Satellite Cloud Phase Estimates*

Cloud products including thermodynamic phase, effective radius, liquid water path, and cloud temperature are derived from GOES Imager data using the visible infrared solar infrared split-window technique (VISST) (Minnis et al., 2001). VISST is a daytime algorithm that requires input from the 0.65, 3.9, 10.8, and 12.0 μm channels. Model calculations of radiances at these channels are produced for 7 liquid and 9 ice crystal size distributions. Cloud properties are retrieved by matching observed radiances to calculations. Because the method relies on visible and infrared radiance measurements, retrieved properties are primarily representative of cloud top conditions.

The VISST method can also be applied to AVHRR data, but does not currently employ the 1.61 μm channel available from daytime AVHRR/3 imagery. The utility of 1.6 μm data for determining cloud phase has been demonstrated by King et al. (1992) and Hutchison (1999). The combination of visible (0.63 μm) and near-infrared (1.61 μm) radiance measurements for estimation of cloud phase provides an additional source of satellite-derived information.

The AVHRR Reflectance Ratio (ARR) method is based on differences in reflection by water and ice at these two wavelengths. Water clouds are highly reflective at 0.63 and 1.61 μm, while ice clouds have a high reflectivity at 0.63 μm and lower reflectivity at 1.61 μm. Cloud phase can be determined using the ratio of reflectances at two wavelengths, where one wavelength is a conservative scatterer for both ice and liquid and the other has strong absorption for ice and weak absorption for liquid. Figure 1 gives an example from the IMPROVE-2 experimental period (November 28, 2001) showing differences in the ratios of reflectance at 1.61 μm to reflectance at 0.63 μm ($R_{1.6/0.6}$) as observed by AVHRR/3. Two clusters of points are apparent. One cluster has high values of $R_{1.6/0.6}$ and relatively warm cloud top temperatures suggesting liquid phase cloud drops, while the other cluster has low values of $R_{1.6/0.6}$ and colder temperatures suggesting ice particles. An empirically derived reflectance ratio threshold of 0.75 separates the two clusters.

The $R_{1.6/0.6}$ threshold that separates liquid and ice phase conditions varies with solar-satellite geometry and particle size. Theoretical calculations of spectral radiances have been performed for a range of particle size distributions, solar-satellite geometries, and cloud optical depths. When applying the ARR method, reflectance ratio for each cloudy pixel is compared with theoretical values to determine whether $R_{1.6/0.6}$ suggests liquid or ice phase. Cloud top temperature derived from AVHRR infrared channels is then considered for each pixel with liquid phase drops. Liquid phase pixels with temperatures below 273 K are designated as containing supercooled liquid. As with the GOES-based VISST method, cloud phase estimates from ARR represent conditions near cloud top.

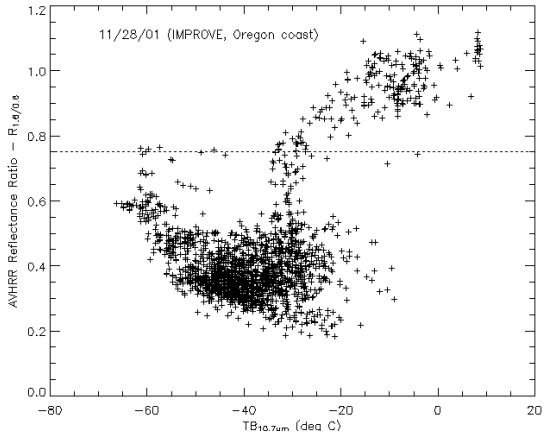

Figure 1: AVHRR reflectance ratio vs. infrared brightness temperature over the IMPROVE-2 study area on November 28, 2001.

4. RESULTS

During IMPROVE-2, the S-Pol radar was used for surveillance of storms moving into northwestern Oregon. When precipitation features of interest made landfall on the Oregon coast, the UW Convair-580 was dispatched and guided into precipitation features. During flights on November 28, 2001 and November 29, 2001, the aircraft encountered supercooled liquid while conducting flight patterns in cloud. Analysis of these cases was undertaken to assess the capabilities of satellite and radar retrieval algorithms to detect supercooled liquid, and to compare the output of the algorithms during coincident observations. To understand the performance of each algorithm in non-icing conditions, a case on December 4, 2001 was also selected for analysis. On this day, a completely glaciated cloud was sampled by the Convair. A summary of the November 28 case study is presented here; other cases will be discussed at the conference.

4.1 Case Study – November 28, 2001

An intense short-wave trough formed over the Pacific Ocean and moved across Oregon between 1200 UTC on November 28 and 0000 UTC on November 29. A surface cyclone and frontal system were associated with this trough. The S-Pol radar showed precipitation across the Oregon Cascades from 0400 UTC on November 28 through 1600 UTC on November 29. Stratiform precipitation was associated with a warm frontal passage. A subsequent cold frontal passage produced a precipitation field containing embedded convective cells.

The Convair conducted microphysical sampling in the S-Pol observational region during the period from 1810-2329 UTC on November 28. Supercooled liquid was noted in flight logs between 2145 and 2200 UTC at an altitude of approximately 4400-5100 m. Retrievals from a ground-based microwave radiometer confirm the presence of liquid in the column. Review of images from the 2D-Cloud probe suggests a mixture of liquid and frozen particles in this time interval, including small spherical particles and some graupel. Other cloud features observed from aircraft are described in Table 1.

Table 1: Summary of aircraft cloud observations for IMPROVE-2 case studies

	Nov 28	**Nov 29**	**Dec 4**
Time of icing observation (UTC)	2145-2200	1815-1915	n/a
Altitude (m)	4400-5100	600-3000	n/a
Cloud top temperature (℃)	-10 to -15	-14	-30 to -35
Phase	mixed	mixed	ice

Cloud phase as derived by VISST from GOES Imager data is shown in Figure 2. Light blue areas represent liquid phase clouds with cloud top temperatures below freezing. Red areas indicate ice phase clouds. Visible imagery suggests a band of high level cirrus corresponding to the ice cloud band that extends across western Oregon. An area of lower-level, liquid phase clouds is situated behind the cirrus band in northwest Oregon. The Convair flight track at this time extended from the location of S-Pol to the southwest, flying primarily in areas designated as supercooled liquid based on VISST estimates.

The ARR estimate of cloud phase based on AVHRR radiances at 2214 UTC results in a similar mixture of supercooled liquid and ice phase cloud tops. $R_{1.6/0.6}$ along the Convair flight track as it flew southwest from the S-Pol location is plotted in Figure 3. Low values near the S-Pol location are indicative of ice phase cloud tops, and probably correspond to times when the aircraft flew under the cirrus cloud layer. Further into the flight track, $R_{1.6/0.6}$ increases and then oscillates about the threshold of 0.7, suggesting the presence of some supercooled liquid, possibly mixed with ice crystals. This result is consistent with in situ measurements from the 2D-Cloud probe.

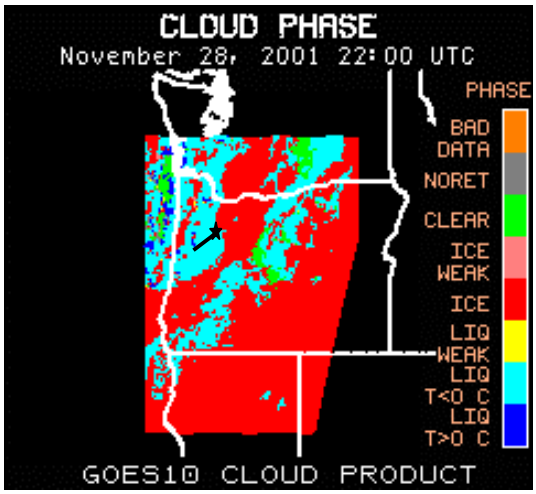

Figure 2: GOES cloud phase product at 2200 UTC on November 28, 2001. Black star shows the location of the S-Pol radar; black line indicates Convair flight track from 2149-2212 UTC.

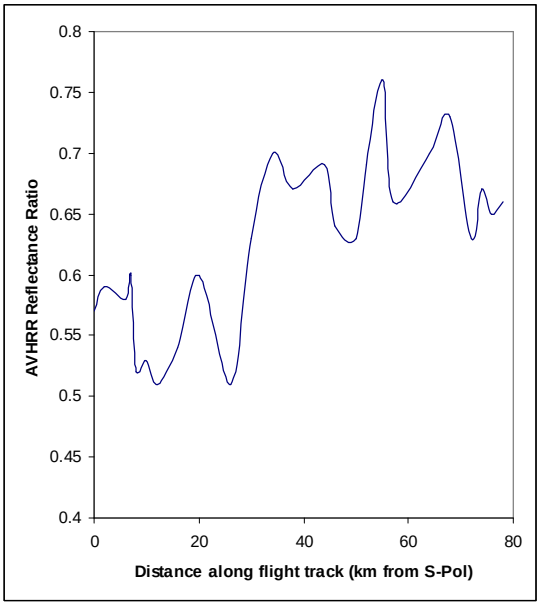

Figure 3: AVHRR reflectance ratio ($R_{1.6/0.6}$) at 2214 UTC on November 28, 2001 along the Convair flight track shown in Figure 2.

Figure 4 shows the S-pol radar vertical cross-section plot along the Convair flight track from 2234-2241 UTC. There are a few intersections of the aircraft with supercooled liquid water (SLW) pixels (orange pixels in Figure 4a). The area of SLW at flight level has a somewhat elevated DZ value of +3 in comparison with similar elevations along the track. Most of the aircraft's intersections are with particles identified as irregular ice crystals (green) and ice crystals. The classification scheme appears to under-identify SLW at this time when compared to flight log observations, but is consistent with in situ 2D-C measurements showing mixed-phase particles. From 2-4 km in altitude, most of the cross-section is filled with wet and dry snow (magenta) particles.

A constant altitude projection of the PID field on November 28 at 2234-2241 UTC is shown in Figure 5. The plot shows the aircraft flight track (solid black line) superimposed on the color-coded PID field at the flight level of 4.5 km. AVHRR reflectance ratio from the 2214 UTC pass is shown as red contours. Areas within the closed contours have values above 0.7 indicating liquid or mixed phase conditions at cloud top according to the satellite retrieval. Values outside the contours (below the 0.7 threshold) indicate ice phase. The radar-estimated SLW pixels (light blue) are clustered mostly in the northwest portion of the region of the plot, which is co-located with a region of mixed-phase $R_{1.6//0.6}$ conditions. The AVHRR and GOES products indicate a large area of liquid or mixed phase conditions situated to the northwest of the radar site (Figures 2 and 3) and moving into the radar's field of view. At 15-30 minutes after this plot, the radar operator's log indicates a cold front passage over the S-Pol site.

Some SLW pixels occur along the aircraft flight track, which is corroborated by aircraft observations of icing. The PID along the southwest portion of the track is mostly ice crystals and irregular ice crystals. Along the northeast part of the track, the PID is mostly ice crystals and snow. The DZ field (figure 4b) shows that the northeast portion of the track had values of 10-20 dBZ where the snow was detected. Most of the SLW pixels had reflectivities in the range of -5 to 5 dBZ. The ZDR field (figure 4c) indicates values close to +0.5 in the region of snow, and average values of about -0.5 dBZ occur where the PID indicates SLW and the ARR indicates mixed phase particles northwest of the aircraft track.

5. Conclusions

Techniques for estimating icing-related cloud properties using radar and satellite data have been applied to case studies derived from IMPROVE-2. Such comparisons of radar and satellite retrievals to aircraft measurements are being used to assess the capabilities of each method for detecting supercooled liquid water in orographic precipitation systems.

Results from one case study described here (and two others to be presented at the conference) show some consistency between the remote and in situ measurements. Cloud thermodynamic phase derivations from GOES Imager (VISST) and AVHRR/3 (ARR) algorithms suggest a combination of mixed- and liquid-phase conditions in two cases where icing conditions were observed by the aircraft, but frozen particles are also present. Radar-derived particle identification (PID) fields are also compared with aircraft in situ and satellite measurements. Ice crystals and irregular ice crystals are the primary particle type detected in the two cases where icing was observed by the aircraft. Due to the mixed-phase conditions, only a few radar pixels indicate the presence of liquid droplets. Perhaps the mere presence of SLW pixels should be a sufficient indicator of icing conditions due to the overlap of SLW, ice crystals and irregular ice crystals in the PID fuzzy logic tables. In a third case where aircraft measurements indicate ice-phase particles exclusively, satellite and radar estimates of phase and particle type also consiste of ice particles.

This limited set of comparisons demonstrates skill in each technique for determining the thermodynamic phase of cloud droplets in mixed phase and glaciated conditions. The comparisons also demonstrate the complimentary value of radar and satellite techniques. Widespread spatial coverage and, in the case of GOES-based retrievals, frequent temporal coverage are obtained from satellite methods. However, these methods provide information near cloud top, so supercooled liquid in lower level cloud layers may not be detected. Radar-based particle detection is still being tested, but may allow for detection of hazardous icing within clouds, as opposed to simply at cloud-top level, albeit over a more limited spatial domain. Ongoing studies will examine additional cases, comparing retrievals in a range of conditions including purely liquid clouds (Politovich et al., 2004).

References

Hutchison, K., 1999: Application of AVHRR/3 imagery for the improved detection of thin cirrus clouds and specification of cloud-top phase, *J. Atm. Oceanic Tech*., 16, 1885-1899.

King, M., Y. Kaufman, W. Menzel, and D. Tanre, 1992: Remote sensing of cloud, aerosol, and water vapor properties from the Moderate Resolution Imaging Spectrometer (MODIS), *IEEE Trans. Geosci. Remote Sens.,* 30, 2-27.

Minnis, P., W.L. Smith, Jr., D.F. Young, L. Nguyen, A.D. Rapp, P.W. Heck, S. Sun-Mack, Q.

Trepte, and Y. chen, 2001: A near-real time method for deriving cloud and radiation properties from satellites for weather and climate studies. Proc. AMS 11th Conf. Satellite Meteorology and Oceanography, Madison, WI, Oct 15-18, 477-480.

Politovich, M., P. Minnis, C. Wolff, J. Haggerty, M. Chapman, P. Heck, and D. Johnson, 2004: Benchmarking the current icing potential algorithm and NASA Langley satellite products, 11th Conference on Aviation, Range, and Aerospace Meteorology, Hyannis, MA, Oct 4-8.

Stoelinga, M. T., P. V. Hobbs, C. F. Mass, J. D. Locatelli, N. A. Bond, B. A. Colle, R. A. Houze, Jr., and A. Rangno, 2003: Improvement of Microphysical Prameterization through Observational Verification Experiment (IMPROVE). *Bull. Amer. Meteor. Soc*., 84, 1807-1826.

Vivekanandan, J., G. Thompson, and T. Lee, 1996: Aircraft icing detection using satellite data and weather forecast model results. FAA Intl. Conf. On Aircraft Icing, Springfield, VA, May 6-8, 1996.

Vivekanandan, J., D. Zrnic, S. Ellis, R. Oye, A. Ryzhkov, and J. Straka, 1999: Cloud microphysics retrieval using S-band dual-polarization radar measurements, *Bull. Amer. Meteorol. Soc.*, 80, 381-388.

Acknowledgments: We thank Kyoko Ikeda for sharing her analysis of Convair 2DC probe data. Mandana Khaiyer provided the GOES cloud products for our case studies. This research is in response to requirements and funding by the Federal Aviation Administration (FAA). The views expressed are those of the authors and do not necessarily represent the official policy or position of the FAA.

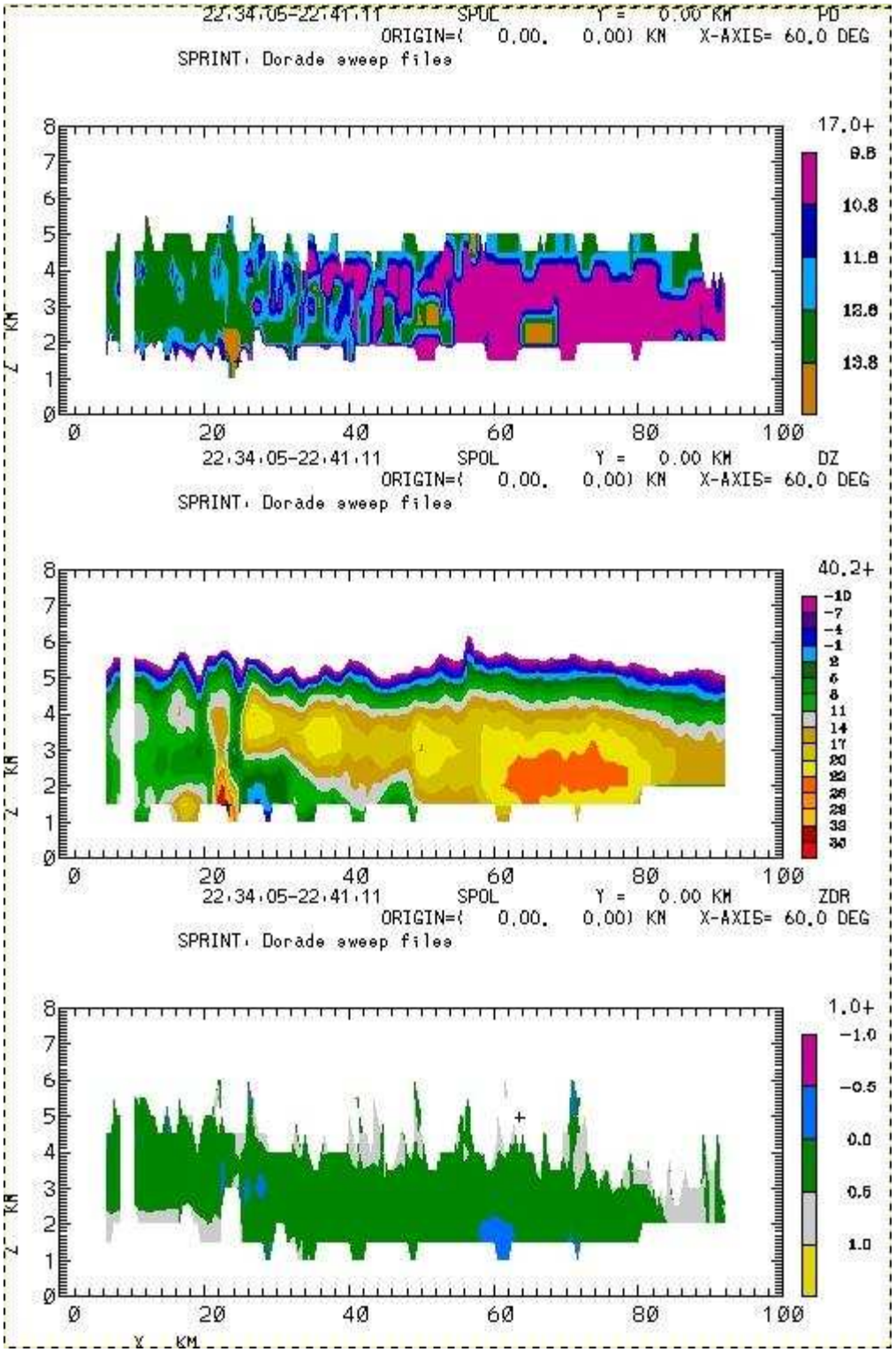

Figure 4: Vertical cross-sections of (a) PID, (b) DZ, and (c) ZDR along the Convair flight track at 2234-2241 UTC on November 28, 2001.

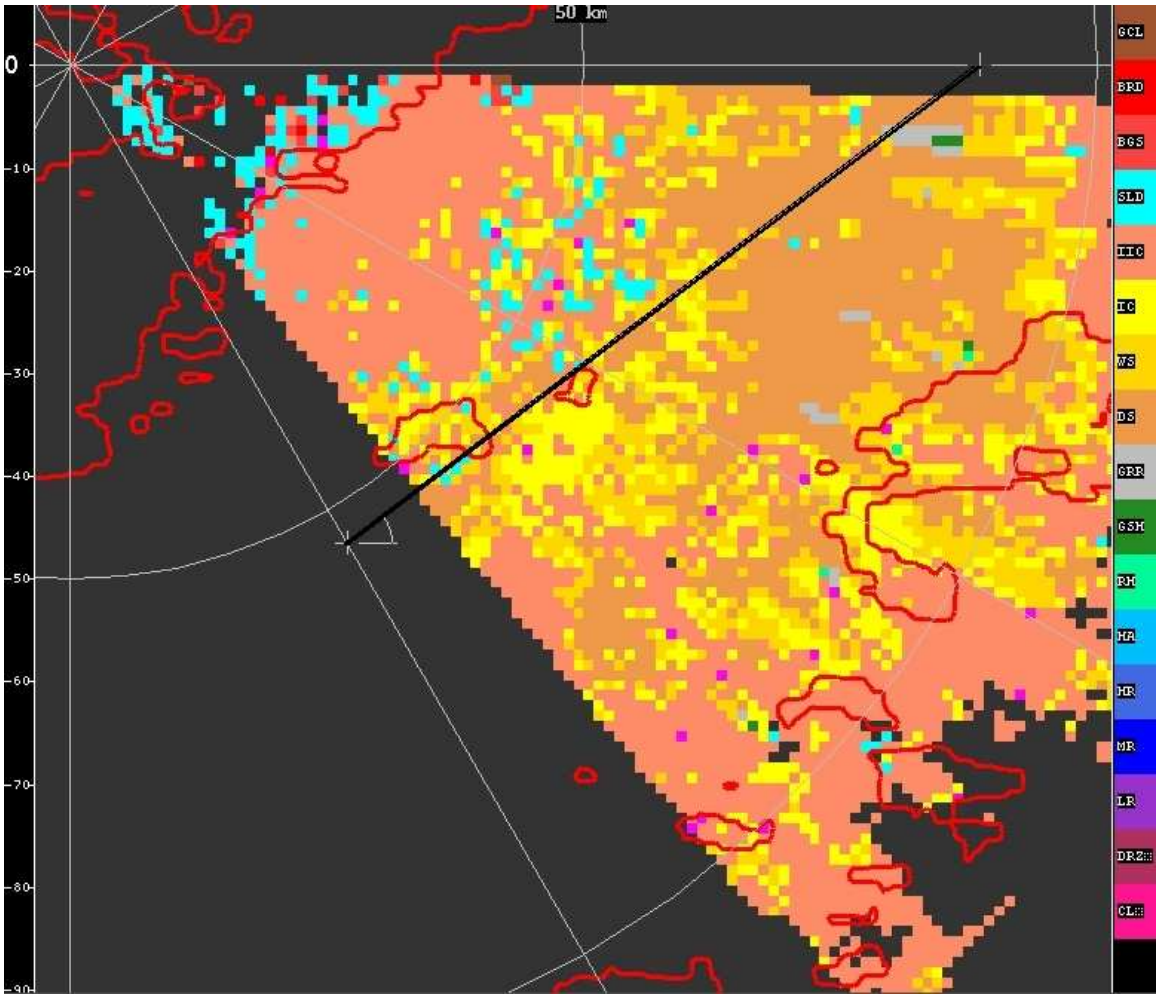

Figure 5: Radar-derived PID (as per colorbar; light blue pixels indicate SLW particles), with AVHRR reflectance ratios superimposed (red contours enclosing values of 0.7 or greater indicate areas of liquid phase) for 2234-2241 UTC on November 28, 2001. The solid black line is the aircraft track. White lines are radar range and azimuth indicators.